

A KINETIC ANALYSIS OF THERMAL DECOMPOSITION OF POLYANILINE/ZrO₂ COMPOSITE

S.-X. Wang¹, Z.-C. Tan^{1,2*}, Y.-S. Li¹, L.-X. Sun² and Y. Li¹

¹College of Environmental Science and Engineering, Dalian Jiaotong University, Dalian 116028, P. R. China

²Thermochemistry Laboratory, Dalian Institute of Chemical Physics, Chinese Academy of Science, Dalian 116023, P. R. China

Synthesis, characterization and thermal analysis of polyaniline (PANI)/ZrO₂ composite and PANI was reported in our early work. In this present, the kinetic analysis of decomposition process for these two materials was performed under non-isothermal conditions. The activation energies were calculated through Friedman and Ozawa–Flynn–Wall methods, and the possible kinetic model functions have been estimated through the multiple linear regression method. The results show that the kinetic models for the decomposition process of PANI/ZrO₂ composite and PANI are all D₃, and the corresponding function is $f(\alpha)=1.5(1-\alpha)^{2/3}[1-(1-\alpha)^{1/3}]-1$. The correlated kinetic parameters are $E_a=112.7\pm 9.2$ kJ mol⁻¹, $\ln A=13.9$ and $E_a=81.8\pm 5.6$ kJ mol⁻¹, $\ln A=8.8$ for PANI/ZrO₂ composite and PANI, respectively.

Keywords: kinetics, PANI, PANI/ZrO₂ composite, thermal decomposition

Introduction

Research in the field of conducting polymers aims mainly at some suitable modification of existing polymers so that their applicability can be improved. Among the different modification techniques available, the one most widely studied and applied in this respect is the formation of composites of different origins. Conducting polymer composites are intimate combinations of one or more inorganic nanoparticles with a polymer so that unique properties of the former can be taken together with the existing qualities of the latter. Over the last few years, conducting polyaniline composites have attracted much attention because they can improve the applicability of polyaniline in different fields, e.g., electrodes of batteries, display devices, immunodiagnostic assay, etc. A lot of literatures have reported their preparation methods, formation mechanism and conductivity property [1–4]. Few concerns [5, 6] have been made on their stability, especially on their kinetics of thermal decomposition. In our early work, we reported the chemical synthesis of PANI/ZrO₂ composite and studied the thermal stability of this composite [7]. In the present work, a kinetic study of thermal decomposition process of PANI/ZrO₂ composite is made. The kinetic parameters of decomposition of this composite have been calculated by employing model-free method and the most probable decomposition mechanism is proposed.

Experimental

Materials and methods

PANI/ZrO₂ composite was chemically synthesized according to the literature method [7]. 1.6 mL aniline was injected to the dispersion of 50 mL of 2 M HCl containing ZrO₂ nanoparticles under ultrasonic action to reduce the aggregation of ZrO₂ nanoparticles. After 30 min, APS was dropped into the above dispersion with constant stirring. The resulting mixture was allowed to react for 10 h at room temperature. The precipitated powder was filtered and washed with HCl and de-ionized water to remove the unreacted aniline monomer and by-products. The product was dried in vacuum at 60°C for 24 h. The molar ratios of aniline to HCl and to APS for either the pure PANI or PANI/ZrO₂ composites were retained at 1:0.5 and 1:1, respectively.

The kinetics of thermal degradation of PANI/ZrO₂ composite for nonisothermal conditions were investigated thermogravimetrically. The thermogravimetric analysis was performed with a Setaram TG model setsys 16/18. The experiments were carried out in air from room temperature to 800°C at various heating rates, which were 5, 10 and 15°C min⁻¹, respectively.

* Author for correspondence: tzc@dicp.ac.cn

Kinetic analysis

Model-free estimation of the activation energy

The equation for kinetic analysis of solid-state decompositions can be expressed as Eq. (1):

$$\frac{d\alpha}{dt} = k(T)f(\alpha) \quad (1)$$

where t is the time and T the temperature and α the extent of conversion. This equation makes the implicit assumption that the temperature dependence of the rate constant, $k(T)$, can be separated from the reaction model, $f(\alpha)$. The explicit temperature dependence of the rate constant is introduced by replacing $k(T)$ with the Arrhenius equation, which gives

$$\frac{d\alpha}{dt} = A \exp\left(\frac{-E}{RT}\right) f(\alpha) \quad (2)$$

where A , E and R are the pre-exponential factor, activation energy and gas constant, respectively. With dynamic techniques, temperature rate dT/dt is set to be a constant β . Thus, the kinetic equation of non-isothermal reaction is obtained as follows:

$$\frac{d\alpha}{dT} = \left(\frac{A}{\beta}\right) \exp\left(\frac{-E_a}{RT}\right) f(\alpha) \quad (3)$$

The non-isothermal methods are called model-free method, which allow the activation energy to be determined as a function of the extent of conversion or temperature without making any assumptions about the reaction model.

FWO method [8] and Friedman method [9] are two representative ones of model-free methods, which are convenient to calculate the activation energy. Figure 1 shows the TG curves of PANI and PANI/ZrO₂ composite (61.9/38.1 (mass/mass)) from

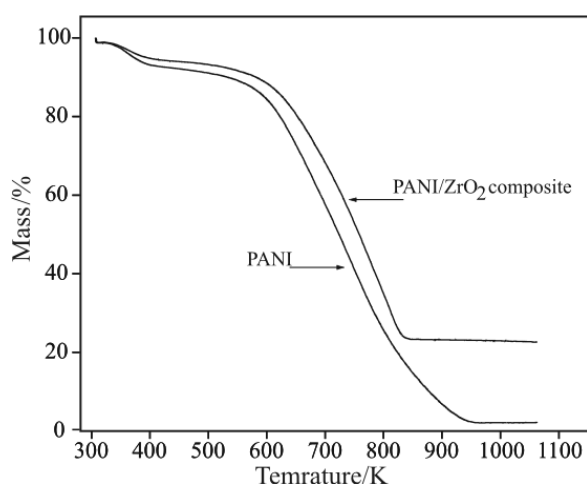


Fig. 1 TG curves of PANI and PANI/ZrO₂ composite (61.9/38.1 (mass/mass)) in air at 10 °C min⁻¹

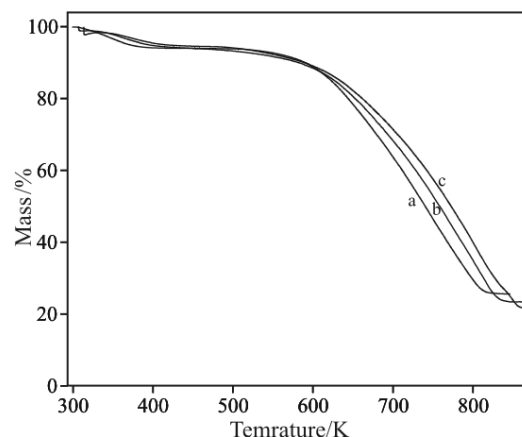


Fig. 2 TG curves of PANI/ZrO₂ composite (61.9/38.1 (mass/mass)) with a – 5, b – 10 and c – 15 °C min⁻¹ heating rates

room temperature to 800 °C with the heating rate of 10 °C min⁻¹. The pure PANI shows two-step mass loss process. The first-step mass loss is attributed to the expulsion of water and dopant (HCl) from the matrix of the PANI. The second-step mass loss is due to the degradation of the PANI chain. The trend of degradation of PANI/ZrO₂ composites is similar to the pure PANI, but thermal stability of the composites has changed. Detailed analysis for this TG curves is shown in our early work [7]. Figure 2 shows the TG curves of PANI/ZrO₂ composite from room temperature to 800 °C with the heating rate of 5, 10 and 15 °C min⁻¹, respectively. It is clearly observed from this figure that the curves shift towards higher temperatures as the heating rate increases. This shift of thermograms to higher temperature with increasing heating rate is expected and is due to a shorter time required for a sample to reach a given temperature at a faster heating rate. The basic data (β , α , T) taken from the TG curves are used in the equations below.

Friedman equation

$$\ln\left[\left(\frac{d\alpha}{dT}\right)\beta\right] = \ln[Af(\alpha)] - \frac{E_a}{RT} \quad (4)$$

Ozawa–Flynn–Wall equation

$$\ln\beta = \left[\frac{AE_a}{RG(\alpha)}\right] - 5.3305 - 1.0516 \frac{E_a}{RT} \quad (5)$$

From Eqs (4) and (5) it is seen that the graphs $\ln(d\alpha/dt)$ vs. $1/T$ and $\ln\beta$ vs. $1/T$ both show straight lines with slopes $m_{(4)} = -E/R$ and $m_{(5)} = -1.052E/R$. The slopes of these straight lines are directly proportional to the reaction activation energy. Some of the Ozawa plots for PANI/ZrO₂ composite are shown in Fig. 3. The fitting straight lines are nearly parallel being an indication that activation energies at the different degree of conversion are similar.

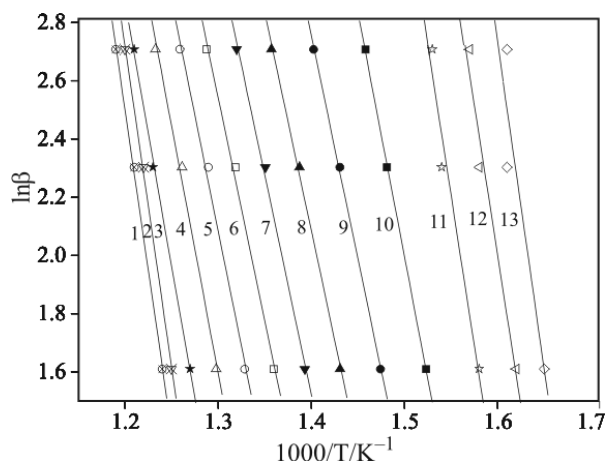


Fig. 3 Ozawa plots of PANI/ZrO₂ composite (61.9/38.1 (mass/mass)) at fractional extent of reaction:
 1 – $\alpha=0.98$; 2 – $\alpha=0.95$; 3 – $\alpha=0.90$; 4 – $\alpha=0.80$;
 5 – $\alpha=0.70$; 6 – $\alpha=0.60$; 7 – $\alpha=0.50$; 8 – $\alpha=0.40$;
 9 – $\alpha=0.30$; 10 – $\alpha=0.20$; 11 – $\alpha=0.10$; 12 – $\alpha=0.05$;
 13 – $\alpha=0.02$

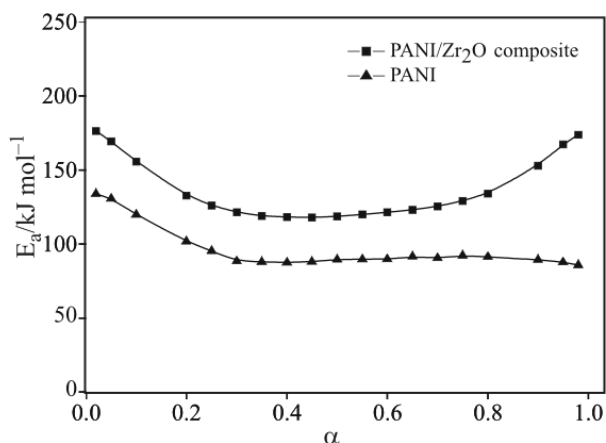


Fig. 4 The dependence of activation energy on the degree of conversion based on OFW method for PANI and PANI/ZrO₂ composite (61.9/38.1 (mass/mass))

Figure 4 gives the dependence of activation energy on the degree of conversion for PANI and PANI/ZrO₂ composite based on OFW method. It is shown that the activation energies of PANI/ZrO₂ composite at different conversion are higher than that of PANI, which indicates that the decomposition is faster and the E_a value is lower. Lower energies are required to make PANI decompose while higher energies are required for the composite. It also can be seen from Fig. 4 that for these two materials, activation energies change little in the range $0.2 \leq \alpha \leq 0.8$. It also suggested that the degradation reaction of PANI and PANI/ZrO₂ composite probably obey a single kinetic mechanism.

Activation energies calculated by OFW and Friedman methods are summarized in Tables 1 and 2

Table 1 Activation energies of PANI using OFW and Friedman methods

| Conversion α | Activation energy/kJ mol ⁻¹ | |
|---------------------|--|-----------------|
| | OFW method | Friedman method |
| 0.20 | 101.8 | 76.6 |
| 0.25 | 95.4 | 72.3 |
| 0.30 | 88.5 | 69.7 |
| 0.35 | 87.9 | 77.7 |
| 0.40 | 87.5 | 80.3 |
| 0.45 | 88.0 | 83.4 |
| 0.50 | 89.5 | 85.3 |
| 0.55 | 89.6 | 85.8 |
| 0.60 | 89.8 | 86.2 |
| 0.65 | 91.6 | 84.7 |
| 0.70 | 90.5 | 81.3 |
| 0.75 | 92.3 | 84.8 |
| 0.80 | 91.4 | 81.3 |
| Average | 91.1±6.7 | 80.7±9.5 |

Table 2 Activation energies of PANI/ZrO₂ composite (61.9/38.1 (mass/mass)) using OFW and Friedman methods

| Conversion α | Activation energy/kJ mol ⁻¹ | |
|---------------------|--|-----------------|
| | OFW method | Friedman method |
| 0.20 | 132.7 | 111.2 |
| 0.25 | 126.0 | 107.0 |
| 0.30 | 121.4 | 106.7 |
| 0.35 | 118.9 | 108.9 |
| 0.40 | 118.2 | 111.7 |
| 0.45 | 117.9 | 113.6 |
| 0.50 | 118.6 | 116.4 |
| 0.55 | 119.9 | 119.5 |
| 0.60 | 121.4 | 122.6 |
| 0.65 | 123.0 | 126.4 |
| 0.70 | 125.3 | 132.3 |
| 0.75 | 129.1 | 142.5 |
| 0.80 | 134.0 | 158.3 |
| Average | 123.6±8.9 | 121.3±11.2 |

for PANI and PANI/ZrO₂ composite respectively. From Tables 1 and 2 it can be seen that activation energies ($0.2 \leq \alpha \leq 0.8$) calculated by using different methods are comparable, which means that the kinetic parameters obtained are reasonable.

Table 3 The selective 15 mechanism functions for evaluation of the kinetic equations

| Name of functions | Kinetics mechanisms | Form of functions | | Symbol |
|----------------------------------|---|---|------------------------------------|--------|
| | | $f(\alpha)$ | $G(\alpha)$ | |
| First order | | $(1-\alpha)$ | | F1 |
| Second order | Formal chemical reaction | $(1-\alpha)^2$ | $(1-\alpha)^{-1}$ | F2 |
| Nth order | | $(1-\alpha)^n$ | $[1-(1-\alpha)^{1-n}]/(1-n)^n$ | Fn |
| Parabola law | One-dimensional diffusion | $0.5\alpha^{-1}$ | α^2 | D1 |
| Valensi equation | Two-dimensional diffusion | $-1/\ln(1-\alpha)$ | $a+(1-\alpha)\ln(1-\alpha)$ | D2 |
| Jander equation | Three-dimensional diffusion | $1.5(1-\alpha)^{2/3}[1-(1-\alpha)^{1/3}]-1$ | $[1-(1-\alpha)^{1/3}]^2$ | D3 |
| Ginstling–Brounshtein | Three-dimensional diffusion | $1.5[(1-\alpha)^{-1/3}-1]^{-1}$ | $((1-2\alpha)/3)-(1-\alpha)^{2/3}$ | D4 |
| Contracting sphere | | $2(1-\alpha)^{1/2}$ | $1-(1-\alpha)^{1/2}$ | R2 |
| Cylindrical symmetry | Phase boundary reaction | $3(1-\alpha)^{2/3}$ | $1-(1-\alpha)^{1/3}$ | R3 |
| Spherical symmetry | Phase boundary reaction | $(1-\alpha)\alpha$ | $\ln\alpha/(1-\alpha)$ | B1 |
| Prout–Tompkins equation | | $(1-\alpha)^n\alpha^a$ | | Bna |
| Expanded Prout–Tompkins equation | Auto-catalysis, Ramifor nucleation | $(1-\alpha)(1+K\alpha)$ | | C1 |
| Avrami–Erofeev equation | Two dimensional nucleation and growth | $(1-\alpha)[- \ln(1-\alpha)]^{1/2}$ | $[- \ln(1-\alpha)]^{1/2}$ | A2 |
| | Three dimensional nucleation and growth | $3(1-\alpha)[- \ln(1-\alpha)]^{2/3}$ | $[- \ln(1-\alpha)]^{1/3}$ | A3 |
| | <i>N</i> -dimensional nucleation and growth | $n(1-\alpha)[- \ln(1-\alpha)]^{(n-1)/n}$ | $[- \ln(1-\alpha)]^{1/n}$ | An |

Table 4 Comparison of the results obtained from the model-fit and the model-free methods for PANI and PANI/ZrO₂ composite (61.9/38.1(mass/mass))

| | PANI | PANI/ZrO ₂ composite |
|--|---|---|
| Activation energy/kJ mol ⁻¹ | | |
| Friedman method | 80.7±9.5 | 121.3±11.2 |
| OFW method | 91.1±6.7 | 123.6±8.9 |
| Model-fitting method | 81.8±5.6 | 112.7±9.2 |
| lnA/s ⁻¹ | 8.8 | 13.9 |
| Reaction type | D ₃ | D ₃ |
| Correlation coefficient | 0.99928 | 0.99849 |
| Function | $f(\alpha)=1.5(1-\alpha)^{2/3}[1-(1-\alpha)^{1/3}]-1$ | $f(\alpha)=1.5(1-\alpha)^{2/3}[1-(1-\alpha)^{1/3}]-1$ |

Determination of kinetic model

Once the activation energy has been determined, it is possible to find the kinetic model which best describes TG curve of the measurement. Fifteen mechanism functions [10] are used to fit kinetic curves. Replacing the data of experiments into the equations corresponding to the fifteen mechanism functions, we used multiple linear regression method to determine the best-fit kinetic model. Generally speaking, the one with highest correlation coefficient (>0.99) is the best-fit kinetic model. The optimized value of activa-

tion energy and lnA was calculated with the best equation. The results are shown in Table 4.

From Table 4, it is seen that the optimized value was close to the value calculated by OFW and Friedman methods. We can conclude that the kinetic model for the decomposition of PANI is D₃, and the corresponding function is $f(\alpha)=1.5(1-\alpha)^{2/3}[1-(1-\alpha)^{1/3}]-1$. The correlated kinetic parameters are $E_a=81.8$ kJ mol⁻¹, lnA=8.8. The kinetic model for the decomposition of PANI/ZrO₂ composite is also D₃. The correlated kinetic parameters are $E_a=112.7$ kJ mol⁻¹, lnA=13.9.

Conclusions

In short, the results of the kinetic analysis above show that the kinetic models for the decomposition process of PANI/ZrO₂ composite and PANI are all D₃, and the corresponding function is $f(\alpha)=1.5(1-\alpha)^{2/3}[1-(1-\alpha)^{1/3}]-1$. The correlated kinetic parameters are $E_a=112.7\pm 9.2$ kJ mol⁻¹, $\ln A=13.9$ and $E_a=81.8\pm 5.6$ kJ mol⁻¹, $\ln A=8.8$ for PANI/ZrO₂ composite and PANI, respectively.

References

- 1 L. J. Zhang and M. X. Wan, *J. Phys. Chem. B*, 107 (2003) 6748.
- 2 Z. M. Zhang and M. X. Wan, *Synth. Met.*, 132 (2003) 205.
- 3 P. S. Khiew, N. M. Huang, S. Radiman and M. S. Ahmad, *Mater. Lett.*, 58 (2004) 516.
- 4 M. Biswas, S. S. Ray and Y. Liu, *Synth. Met.*, 105 (1999) 99.
- 5 D. Tsocheva and L. Terlemezyan, *J. Therm. Anal. Cal.*, 81 (2005) 3.
- 6 S. X. Wang, L. X. Sun, Z. C. Tan, F. Xu and Y. S. Li, *J. Therm. Anal. Cal.*, 89 (2007) 609.
- 7 S. X. Wang, Z. C. Tan, Y. S. Li, L. X. Sun and T. Zhang, *Thermochim. Acta*, 441 (2006) 191.
- 8 H. L. Friedman, *J. Polym. Sci. Part C*, 6 (1963) 183.
- 9 T. Ozawa, *Bull. Chem. Soc. Jpn.*, 38 (1965) 1881.
- 10 L. Jun, *Thermochim. Acta*, 406 (2003) 77.

Received: January 25, 2007

Accepted: August 18, 2007

DOI: 10.1007/s10973-007-8356-5